AGU PUBLICATIONS

JGR

Journal of Geophysical Research: Solid Earth

RESEARCH ARTICLE
10.1002/2014JB011290

Key Points:
- Methane hydrates are destabilizing beneath >5000 km^2 of Beaufort Sea upper slope
- Recent upper ocean temperature warming is causing hydrate instability
- Complex heat flow exists beneath the U. S. Beaufort continental margin

Supporting Information:
- Readme
- Text S1
- Table S1
- Figure S1

Correspondence to:
B. J. Phrampus,
bphrampus@smu.edu

Citation:
Phrampus, B. J., M. J. Hornbach, C. D. Ruppel, and P. E. Hart (2014), Widespread gas hydrate instability on the upper U.S. Beaufort margin, *J. Geophys. Res. Solid Earth*, *119*, 8594–8609, doi:10.1002/2014JB011290.

Received 15 MAY 2014
Accepted 28 OCT 2014
Accepted article online 5 NOV 2014
Published online 9 DEC 2014

Widespread gas hydrate instability on the upper U.S. Beaufort margin

Benjamin J. Phrampus[1], Matthew J. Hornbach[1], Carolyn D. Ruppel[2], and Patrick E. Hart[3]

[1]Huffington Department of Earth Sciences, Southern Methodist University, Dallas, Texas, USA, [2]U.S. Geological Survey, Woods Hole, Massachusetts, USA, [3]U.S. Geological Survey, Menlo Park, California, USA

Abstract The most climate-sensitive methane hydrate deposits occur on upper continental slopes at depths close to the minimum pressure and maximum temperature for gas hydrate stability. At these water depths, small perturbations in intermediate ocean water temperatures can lead to gas hydrate dissociation. The Arctic Ocean has experienced more dramatic warming than lower latitudes, but observational data have not been used to study the interplay between upper slope gas hydrates and warming ocean waters. Here we use (a) legacy seismic data that constrain upper slope gas hydrate distributions on the U.S. Beaufort Sea margin, (b) Alaskan North Slope borehole data and offshore thermal gradients determined from gas hydrate stability zone thickness to infer regional heat flow, and (c) 1088 direct measurements to characterize multidecadal intermediate ocean warming in the U.S. Beaufort Sea. Combining these data with a three-dimensional thermal model shows that the observed gas hydrate stability zone is too deep by 100 to 250 m. The disparity can be partially attributed to several processes, but the most important is the reequilibration (thinning) of gas hydrates in response to significant (~0.5°C at 2σ certainty) warming of intermediate ocean temperatures over 39 years in a depth range that brackets the upper slope extent of the gas hydrate stability zone. Even in the absence of additional ocean warming, 0.44 to 2.2 Gt of methane could be released from reequilibrating gas hydrates into the sediments underlying an area of ~5–7.5 × 10^3 km^2 on the U.S. Beaufort Sea upper slope during the next century.

1. Introduction

Methane hydrates, ice-like solids that consist of methane and water that are stable at moderate pressures and low temperatures, are believed to be widespread in Arctic Ocean continental slope and rise sediments [e.g., *Kvenvolden and Grantz*, 1990; *Biastoch et al*., 2011; *Reagan et al*., 2011]. The Arctic Ocean and surrounding landmasses have experienced rapid warming on short-term (decadal) time scales [e.g., *Johannessen et al*., 2004]. On longer time scales, warming of more than 10°C since the Last Glacial Maximum (LGM) has been linked to permafrost thaw, reduced Arctic Ocean sea ice cover and possibly methane hydrate destabilization [*Brigham and Miller*, 1983; *Allen et al*., 1988; *Paull et al*., 2007; *Shakhova et al*., 2010]. In the marine system, the impingement of warming ocean waters on continental slopes, which host the most climate-sensitive gas hydrate deposits [*Kvenvolden*, 1993; *Ruppel*, 2011], not only leads to breakdown (dissociation) of gas hydrates into constituent methane and water but also can increase subsurface fluid pressures and reduce slope stability [e.g., *Kayen and Lee*, 1991; *Flemings et al*., 2003; *Hornbach et al*., 2004]. Methane that migrates to the seafloor after dissociation may be released into the ocean, enhancing water column methane oxidation that leads to increased ocean acidification and deoxygenation [*Kvenvolden*, 1988; *Dickens et al*., 1995; *Archer*, 2007; *Camilli et al*., 2010; *Biastoch et al*., 2011]. Due to the potential for methane destabilization and release, unraveling the connections between climate warming and methane hydrate dynamics on the Beaufort Sea margin has important implications for marine sediment mechanics, Arctic Ocean chemistry, and possibly atmospheric greenhouse gas concentrations.

In typical deepwater marine gas hydrate systems, gas hydrates can in theory exist at the seafloor. In practice, outside seep areas, gas hydrate does not usually occur as shallow as the seafloor because anaerobic methane oxidation processes within the sulfate reduction zone that lies within the uppermost meters of sediments consume most of the methane [*Reeburgh*, 2007]. To first order, the base of gas hydrate stability (BGHS) is controlled by the geothermal gradient and hydrostatic pressure within the saturated and generally high-porosity sediments that make up the uppermost hundreds of meters on most continental margins. The BGHS often manifests in seismic data as a strong, reverse-polarity bottom-simulating seismic reflector (BSR) [*Shipley*

et al., 1979; *Kvenvolden and Grantz*, 1990; *Andreassen et al*., 1997]. The negative impedance contrast at the BSR reflects the layering of higher-velocity, hydrate-bearing sediments over lower-velocity, gas-charged sediments [*Holbrook et al*., 1996]. The presence of a BSR is a sufficient condition for the likely occurrence of gas hydrate in sediments, but gas hydrate sometimes exists without an underlying BSR [*Holbrook et al*., 1996]. BSR depths, combined with hydrate stability models [*Sloan and Koh*, 2008], have long been used to constrain subsurface temperature regimes [*Yamano et al*., 1982] and to assess the degree to which the sediments are in steady state thermal equilibrium [e.g., *Ruppel*, 1997; *Ruppel and Kinoshita*, 2000; *Hornbach et al*., 2004; *Hornbach et al*., 2008; *Phrampus and Hornbach*, 2012]. Where the gas hydrate stability zone (GHSZ) is out of equilibrium with contemporary ocean temperature and heat flow conditions, the contemporary distribution of gas hydrates may sometimes reflect past conditions. Future adjustments in the distribution of gas hydrates would be expected to bring the system back into equilibrium.

In this study, we use the regional 1977 ocean temperature data, long-term ocean temperature data, and heat flow observations combined with numerical models to predict the steady state location of the GHSZ in the U.S. Beaufort Sea. We then compare modeled steady state GHSZ with direct observations of BSRs revealed in regional seismic data. The results allow us to delineate where methane hydrates may be destabilizing on the U.S. Beaufort continental margin.

2. Setting

The study area is the continental slope of the U.S. part of the Beaufort Sea, roughly between the shelf break (~100 m water depth) on the south and the continental rise (~3000 m water depth) on the north. The region stretches ~600 km from the offshore extension of the U.S.-Canada border (141st meridian west) on the east to Barrow, Alaska, on the west. To date, no comprehensive methane hydrate stability analysis has been conducted along this margin.

Owing to differences in data availability, the number of past studies, and the geologic, structural, glacial, sea level, and sedimentation histories, we focus only on the U.S. part of the Beaufort Sea margin. Our results are likely not fully applicable to the Beaufort Sea offshore Canada, which differs from the U.S. part of the margin in having experienced Laurentide glaciation [*Dyke and Prest*, 1987], strong sedimentary influence of the Mackenzie River [*Carmack et al*., 1989], a petroleum system history that has left the shelf sediments charged with gas [*Blasco et al*., 2011], and active compressive deformation [*Houseknecht et al*., 2012].

West of Flaxman Island on the U.S. Beaufort Sea margin, the continental slope is a rifted margin terrace that overlies increasingly attenuated continental crust as the base of the continental slope transitions into the Canada Basin. Along this part of the Beaufort Sea, the Brooks Range fold and thrust belt lie well inland and is bordered to the north by the wide North Slope coastal plain (Colville foreland) and a classic passive margin offshore. Near the Canning River, the fold and thrust belt curve northward and then veer east, finally intersecting the present-day coastline near the U.S.-Canada border. The Beaufort shelf and continental slope east of the Canning River is part of the Canning-Mackenzie deformed margin (CMDM), most of which lies within Canadian waters. Offshore, the CMDM is characterized by folding [*Houseknecht et al*., 2012], mud diapirism, and pingo-like features [*Paull et al*., 2007; *Blasco et al*., 2011; *Hart et al*., 2011].

The large-scale tectonics—typical passive margin on the west transitioning to a passive margin undergoing active compression on the east—is reflected in the morphology of the continental slope, where most gas hydrate discussed in this study occurs. North of Prudhoe Bay, the continental slope is steep, deepening by 900 m over a distance of ~11 km (4.7° average slope), compared to the shallower slope (~1.4°) off the Canning River region (Figure 1). The steep continental slope north of Prudhoe Bay occurs where the passive margin province begins to transition eastward to the CMDM. The wider, gentler continental slope within the CMDM is where the connection between large-scale slope failures and gas hydrate/gas-charged sediments was first investigated [*Kayen and Lee*, 1991]. Close to the seafloor, this area has also been most strongly affected by glacial scouring associated with a floating ice sheet that may have extended from the Amundsen Gulf across the Beaufort Sea to the Chukchi Plateau during late Pleistocene glaciation [e.g., *Engels et al*., 2008].

This study focuses on the deepwater gas hydrate system within the continental slope and rise of the U.S. Beaufort Sea. In this area, most of the sedimentary section is Cenozoic, progradational, postrift, and clastic prism deposits from the Brooks Range and Arctic Foothills [*Grantz et al*., 1990; *Houseknecht and Bird*, 2011],

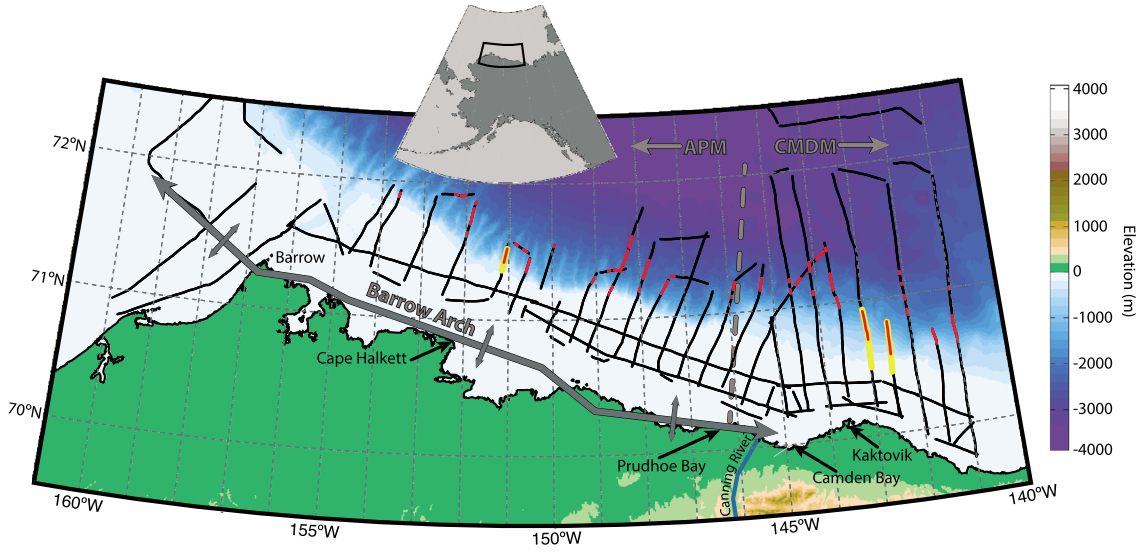

Figure 1. U.S. Beaufort Sea study area with key geologic features including the Barrow Arch, Alaskan passive margin, and Canning-Mackenzie deformed margin (CMDM) [*Houseknecht and Bird*, 2006]. Seismic lines from the 1977 USGS surveys are shown in black [*Andreassen et al.*, 1995]. The red represents the minimum extent of BSRs in the Beaufort Sea based on seismic interpretations. The seismic lines that most clearly reveal dynamic (nonsteady state) hydrate stability zones are shown in bold yellow. These lines are 767, 718, and 730 from west to east, respectively.

with additional sediment derived from the ancestral Mackenzie River to the east [*Houseknecht et al.*, 2012]. The sediments form a seaward thickening wedge that mantles the pre-Mississippian Beaufort rift shoulder and the prerift and synrift deposits associated with opening of the Canada Basin [*Houseknecht et al.*, 2012].

The shelf (<100 m water depth) in the study area did not undergo continental glaciation during the LGM but was instead exposed subaerially during the sea level lowstand [*Dyke et al.*, 2002]. This led to the formation of permafrost and possibly permafrost-associated gas hydrate in the sediments that now comprise the shelf. During subsequent sea level rise of 100 m or more, the permafrost and gas hydrate has probably mostly thawed, and recent seismic analyses indicate that permafrost probably does not remain beyond ~30 km (~20 m isobath) from the present-day coastline [*Brothers et al.*, 2012]. Permafrost-associated gas hydrates, which are not known to form BSRs and whose existence on the U.S. Beaufort Sea shelf is probably not widespread, are not considered in this study.

Sea level rise of 100 m or more since the late Pleistocene has played an important role not only on the continental shelf but also on the U.S. Beaufort Sea upper slope (~100 to 500 m water depth). The upper slope lay close to the late Pleistocene shoreline and may have been the locus of deltaic sedimentation from ancestral rivers and deposition from the Brooks Range into the early Holocene [*Grantz et al.*, 1990]. During the latter part of the Holocene, much of the central and eastern parts of the margin have been sediment starved. The Colville River is the only large river on the U.S. Beaufort Sea coastline, but its annual discharge and sediment load are a fraction of those of the Mackenzie River or the great rivers of the Siberian arctic. A branch of the Mackenzie River sediment plume sometimes veers west across the Beaufort Sea upper slope, providing enhanced sediment loads.

The extent of deepwater gas hydrates on the U.S. Beaufort continental slope and rise was first mapped in 1977 by the U.S. Geological Survey (USGS), which used multichannel seismic (MCS) data along 24 lines to delineate BSRs, building on the results of earlier, single-channel surveys [*Grantz et al.*, 1976]. The 1977 MCS data were acquired with a 2400 m long streamer and a five air gun, 22,700 cm^3 array [*Grantz et al.*, 1982; *Andreassen et al.*, 1995]. Data are 24-fold with a trace spacing of 50 m. Velocity uncertainty increases with depth in the seismic data set, reaching ±12.7% at the deepest observed BSR. In these data, the BSR could be identified in 80% of the ~40,000 km^2 gas hydrate province [*Grantz et al.*, 1976; *Kvenvolden and Grantz*, 1990; *Andreassen et al.*, 1995]. Starting at ~350 m below sea level (mbsl) on the upper continental slope, the GHSZ thickens seaward, with the BSR reaching ~770 m below seafloor (mbsf) at 3200 mbsl.

3. Data and Methods

Determining the steady state morphology of the GHSZ in the Beaufort Sea requires constraints on the two key boundary conditions that control the stability of gas hydrates at any given depth: bottom water temperature (BWT) and regional heat flow. Currently, heat flow is poorly constrained in the Beaufort Sea, and ocean temperatures, although well constrained from water column conductivity-temperature-depth (CTD) data, are warming with time [*Melling*, 1998]. Below, we describe the methods used to constrain both ocean temperature and regional heat flow to develop a steady state gas hydrate stability model for the Beaufort Sea that we then compare with the 1977 USGS seismic observations.

3.1. Ocean Temperature

Accurately predicting the thickness of the GHSZ requires a clear understanding of ocean temperature with depth. Using the World Ocean Database [*Levitus et al*., 1998], we extracted 1088 CTD casts collected in the study area (Figure 2a). Most of the CTD data were acquired during two annual periods between calendar days 50 and 150 (winter-spring) and 200 and 300 (summer-fall; Figure 2b). CTD data exist from 1976 to 2008 for the winter-spring period and from 1971 to 2010 for summer-fall period. For shallow water depths (≤200 mbsl), consistent CTD data extend back 39 years in the summer-fall. For deeper depths (≥300 mbsl), a maximum of 25 years of CTD data is available. Within these constraints, we calculate seasonal average ocean temperatures with depth.

We analyzed raw data from 100 to 1000 mbsl at 5 m intervals for each of the 1088 CTD casts to generate averages. To reduce the potential for systematic error with temperature at each depth, we determine the average and standard deviation temperature value in each interval by averaging all values within a ±5 m depth range. We then combine all results for each year and calculate an average temperature and standard deviation (example in Figure 3). This produces an estimate and standard deviation of winter-spring/summer-fall ocean temperature with depth for each year.

Finally, we calculate a mean and standard deviation long-term (up to 39 years) annual rate of temperature change in the Beaufort Sea at each depth interval by using Monte Carlo simulations that incorporate our measured annual temperature-depth values and associated uncertainties. To initiate the Monte Carlo simulation, we choose a random average yearly temperature within the normally distributed error at each depth for each year. We then run Monte Carlo simulations through 1000 realizations in which each realization uses a least squares approach to estimate the slope (i.e., linear rate of temperature change) that best fits the annual temperature variation with depth. From these results, we determine the average temperature variation for each depth, for each year, for all past years. This produces a plot of linear changes in ocean temperatures for the winter-spring and summer-fall time periods (Figure 4).

The result generally matches other ocean temperature observations that indicate steady ocean temperature warming at intermediate water depths in the Beaufort Sea [e.g., *Melling*, 1998]. We determine the average yearly temperature change by calculating the statistical mean and standard deviation of the winter-spring and summer-fall temperature changes, assuming that the winter-spring and summer-fall temperature changes each represent 50% of the data set. This approach removes bias introduced due to the summer-fall sample count greatly outnumbering the winter-spring sample count. The result represents the average rate of linear temperature change along the Beaufort continental margin and reveals that the dominant change in ocean temperatures occurs at ~300–550 mbsl (Figure 4). Below 550 mbsl, we see no statistically significant evidence for ocean temperature change across the region.

3.2. Heat Flow

Developing a model that estimates the depth to the base of methane hydrate stability also requires regional constraints on heat flow. Thirty-four terrestrial heat flow measurements are available from borehole measurements on the North Slope of Alaska (Figure 5 and Table S1 in the supporting information) [*Lachenbruch and Marshall*, 1969; *Lachenbruch et al*., 1982; *Deming et al*., 1992]. Offshore, heat flow can be inferred only indirectly [e.g., *Houseknecht and Bird*, 2011]. In the U.S. Beaufort Sea, wells are almost exclusively in the coastal zone, with only a few wells drilled on the middle to outer shelf and none on the upper continental slope. None of the offshore wells has publicly available data that constrain thermal regimes in the uppermost hundreds of meters of sediment. However, one well (Aurora) located ~6 km from shore on the central U.S. Beaufort coast provides thermal gradient data at depths >300 mbsl (Figure 5 and Table S1 in the supporting information) [*Paul*, 1994]. Given the paucity of offshore data, we rely on both onshore thermal

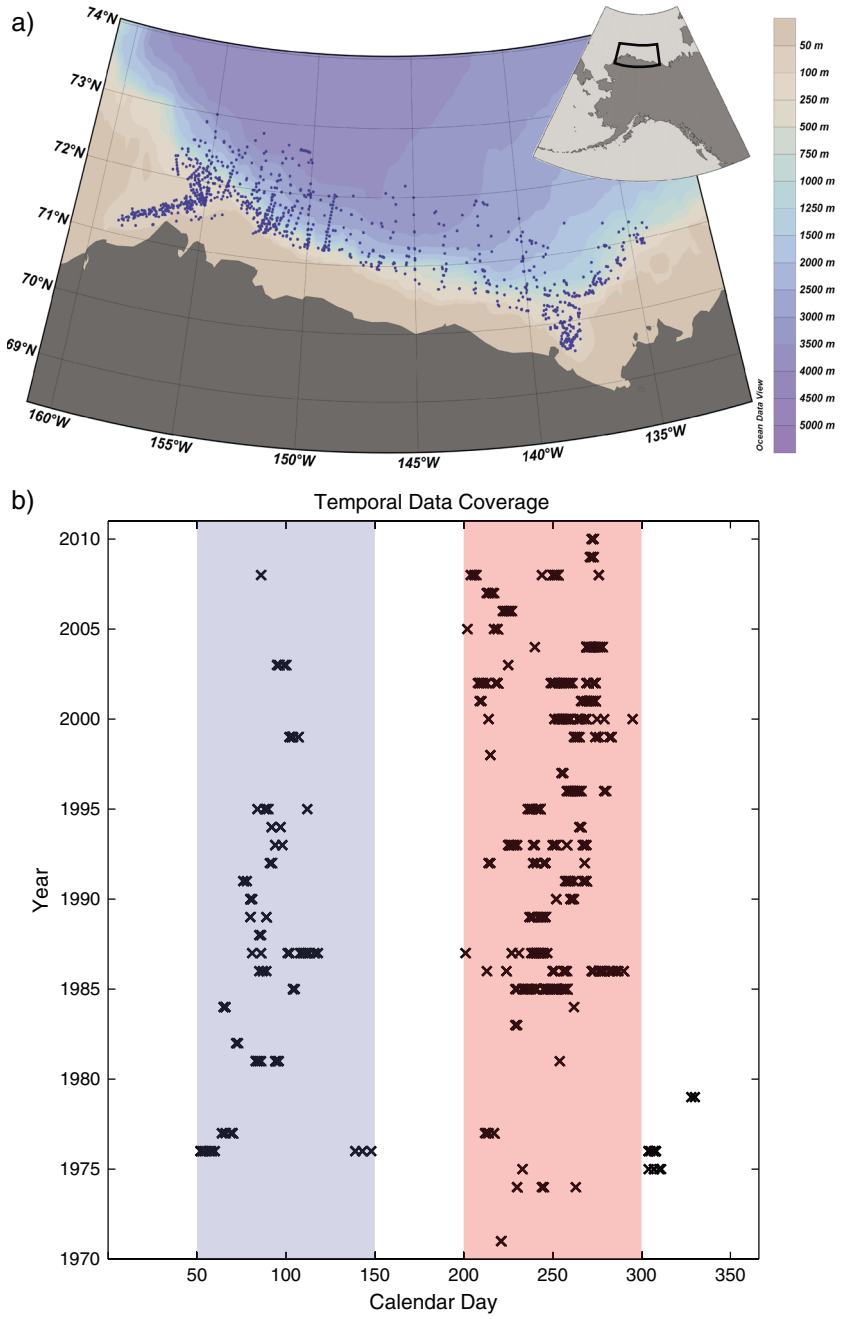

Figure 2. (a) Bathymetric map of study area with the location of 1088 CTD stations shown in blue. (b) Plot showing the day of the year each of the 1088 CTDs were collected. This study analyzes data between calendar days 50–150 (blue) and 200–300 (red), which have the highest data density.

data and constraints based on the depth of deepwater (>1000 mbsl) BSRs to constrain regional heat flow. Previous studies indicate that ocean temperatures at depths greater than 1000 mbsl have experienced no significant change within the last 5000–10,000 years, consistent with our own analysis of CTD data for up to 39 years [e.g., *Waelbroeck et al*., 2002; *Westbrook et al*., 2009; *Marín-Moreno et al*., 2013]. This implies that deepwater BSRs represent a useful tool for estimating first-order heat flow in the deepwater Beaufort Sea.

The compiled heat flow map is shown in Figure 5. Such an interpolated heat flow map has inherent weaknesses since it combines onshore and offshore areas that have different geologic, cryospheric, tectonic, subsidence, and thermal histories and interpolates values between onshore and deepwater areas, directly

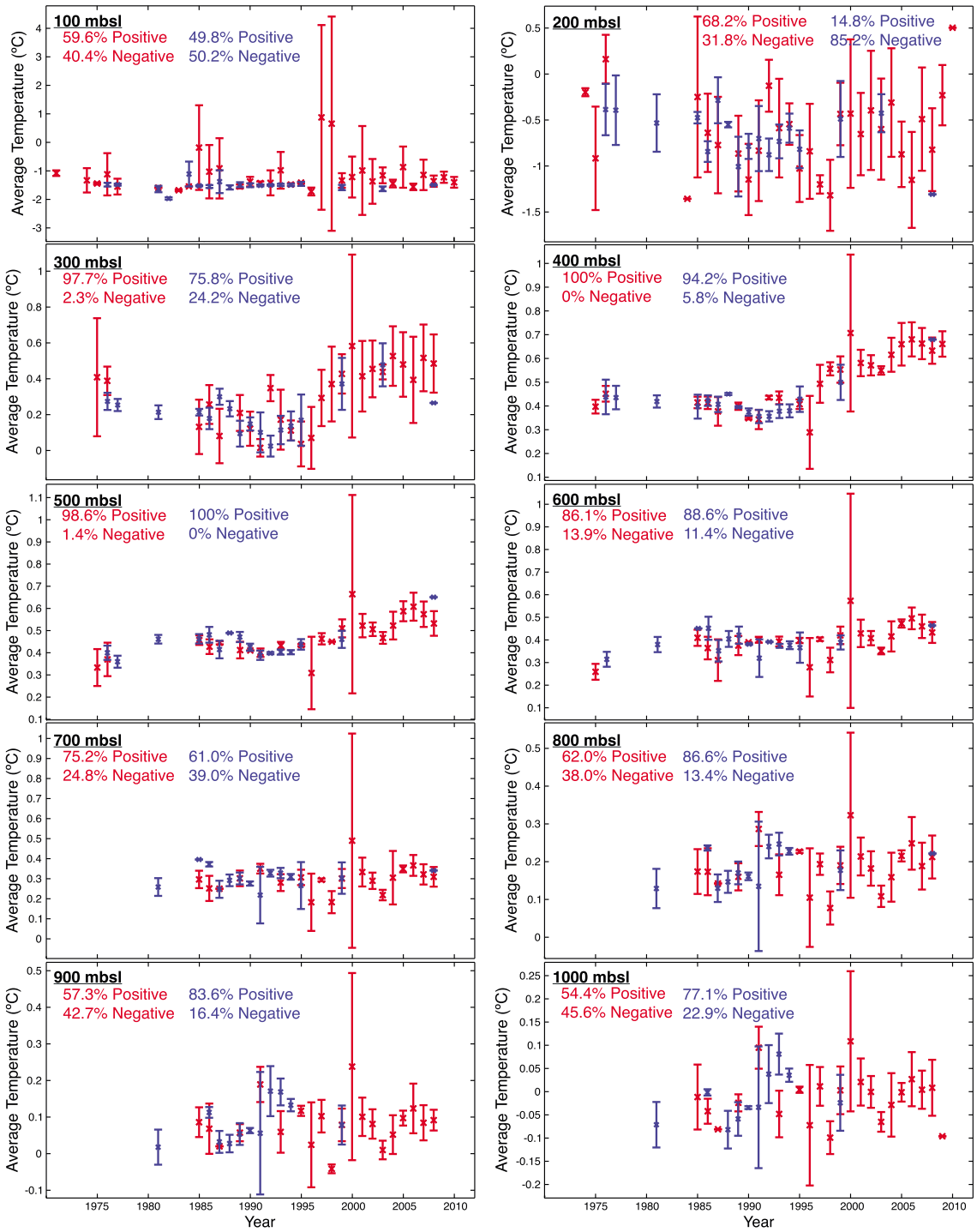

Figure 3. Plot of average temperatures per year at each depth interval with 1 sigma error plotted for each year for the summer-fall (red) and winter-spring (blue) time frames. Temperature limits (*y* axis) are not equal for each plot. Percentages represent the total percent of positive and negative slopes obtained during the Monte Carlo simulation, implying either average temperature warming or cooling, respectively, for the past 25–39 years at each depth interval.

across the shelf. Along much of this margin, the map is also interpolated across the Beaufort hingeline, the crest of which is known as the Barrow Arch. This structural feature runs near the coastline for hundreds of kilometers and acts as an important boundary for some sedimentary and petroleum systems (Figure 1) [*Houseknecht and Bird*, 2006]. Our analysis therefore represent only a first-order approach to assessing heat flow in the Beaufort Sea and has large uncertainties that we quantify below.

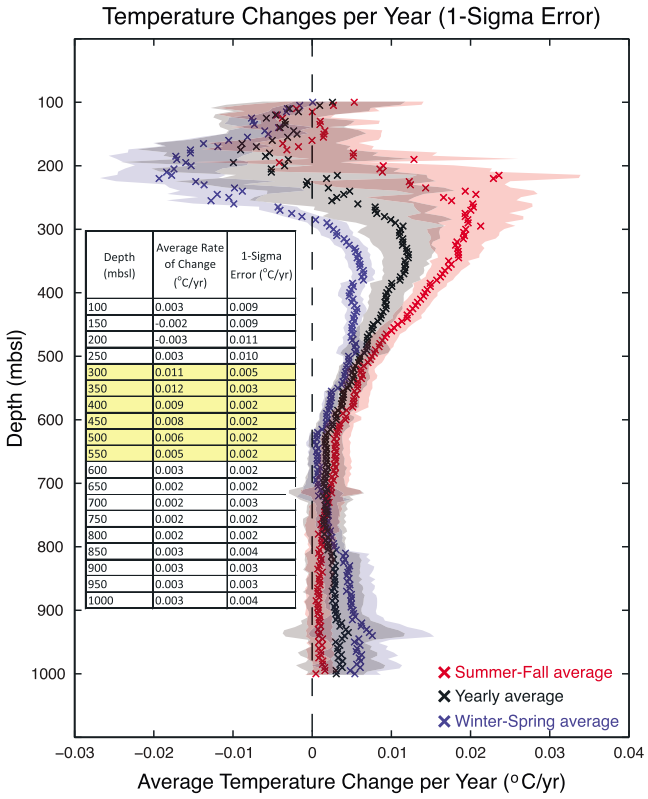

Depth (mbsl)	Average Rate of Change (°C/yr)	1-Sigma Error (°C/yr)
100	0.003	0.009
150	-0.002	0.009
200	-0.003	0.011
250	0.003	0.010
300	0.011	0.005
350	0.012	0.003
400	0.009	0.002
450	0.008	0.002
500	0.006	0.002
550	0.005	0.002
600	0.003	0.002
650	0.002	0.002
700	0.002	0.003
750	0.002	0.002
800	0.002	0.002
850	0.003	0.004
900	0.003	0.003
950	0.003	0.003
1000	0.003	0.004

Figure 4. Plot of the average linear change in temperature over the 25–39 year time frame with 1 sigma error estimations resulting from the Monte Carlo simulations in the shaded regions. The different colors represent the different seasons (winter versus summer), with the black data representing the statistical average yearly variations in ocean temperatures. The table shows the numerical data represented by the yearly (black) data in the figure.

3.2.1. Terrestrial Heat Flow

A database of terrestrial heat flow measurements has been developed for the Alaskan North Slope, an area generally characterized by continuous permafrost hundreds of meters thick [*Osterkamp and Payne*, 1981; *Osterkamp et al.*, 1985; *Collett et al.*, 1988]. For this reason, we focus on conductive heat flow instead of thermal gradients, which are strongly affected by the unique thermal conductivity structure of permafrost sediments. *Deming et al.* [1992] used boreholes to obtain 27 North Slope heat flow measurements with an average uncertainty of ±19 mW/m^2 (Table S1 in the supporting information). *Lachenbruch et al.* [1982] used observation wells and drill cuttings to determine an average heat flow of ~55 ± 6 mW/m^2 in the Prudhoe Bay region, with an additional two wells described by *Lachenbruch and Marshall* [1969] having unknown uncertainty (Table S1 in the supporting information). Taken together, the data reveal variable heat flow across the Alaskan North Slope, which encompasses a range of lithologies, petroleum systems, and tectonic settings [*Houseknecht and Bird*, 2011].

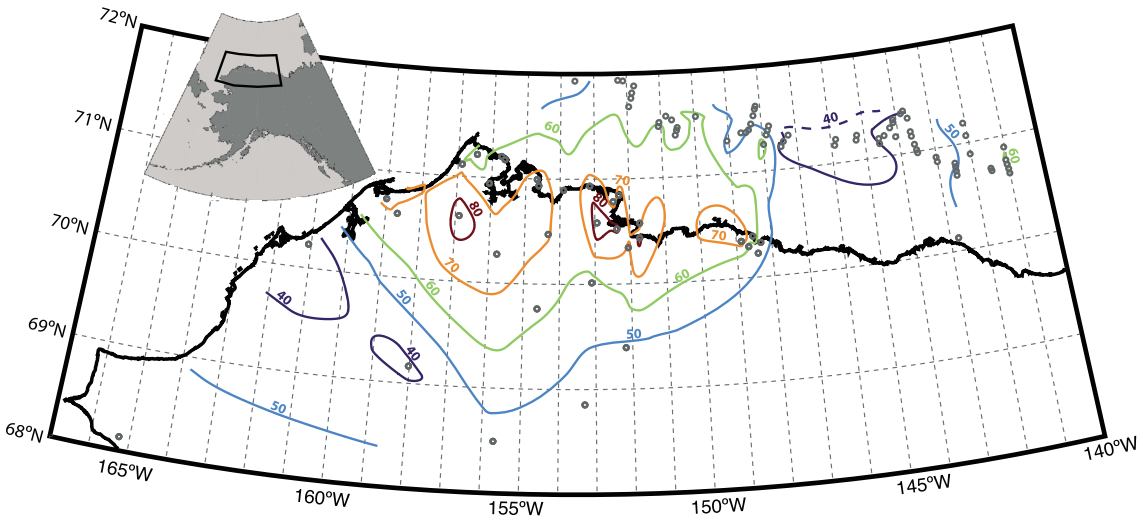

Figure 5. Regional heat flow map created by integrating previously published land heat flow data [*Lachenbruch and Marshall*, 1969; *Lachenbruch et al.*, 1982; *Deming et al.*, 1992] with heat flow estimations using deepwater (>1000 mbsl) BSRs [*Yamano et al.*, 1982]. Each dot represents a heat flow estimation with variable error (Table S1 in the supporting information).

3.2.2. Deepwater Heat Flow

We use BSR depths extracted from legacy USGS seismic data [*Grantz et al*., 1982] to constrain thermal gradients and infer heat flow in the uppermost part of the sedimentary section, following the method of *Yamano et al*. [1982]. The seafloor boundary condition (bottom water temperature) is constrained using existing databases of oceanographic measurements (section 3.1). The BSR temperature T is determined using standard stability models for pure methane [*Sloan and Koh*, 2008] and assuming hydrostatic pressure at subseafloor depth z of the BSR. Heat flow q is calculated from

$$q = k\frac{dT}{dz} \tag{1}$$

where dT/dz denotes the geothermal gradient and and k is the thermal conductivity. BSRs at midslope water depths on the U.S. Beaufort margin are continuous and smooth, showing no evidence of warping due to significant fluid advection. We therefore assume that regional heat flow is dominated by conduction, consistent with heat transfer at other continental margin locations where continuous BSRs exist [e.g., *Yamano et al*., 1982; *Ruppel et al*., 1995].

Ocean water temperatures are constrained using data from 76 CTD casts that were conducted in 1977 (the year of the seismic data acquisition) and extracted from the World Ocean Database [*Levitus et al*., 1998]. BSR depths are determined from the legacy USGS MCS data. We identified the BSR as a reverse-polarity reflector in migrated USGS seismic data and confirmed the location of BSRs via interval velocity analysis, with lower seismic velocities observed below BSRs compared to higher velocities in the overlying GHSZ [e.g., *Holbrook et al*., 1996].

Uncertainty in BSR depths propagates into heat flow uncertainty, and we account for this via statistical analysis of interval velocities obtained from 1977 USGS common midpoint gathers. Interval velocities have increasing error with depth [*Dix*, 1955]. Not surprisingly, we find that BSR depth uncertainty using interval velocities depends upon BSR depth below the seafloor, with higher uncertainty at deeper BSR depths due to the additive nature of interval velocity errors. Specifically, we find the greatest depth uncertainty of approximately ±50 m occurs at the greatest depths (>1000 mbsf). For shallow BSRs along the upper continental slope, depth uncertainty is significantly lower (±15–20 m).

With BSR depth and seafloor temperature constrained, we estimate heat flow by calculating the temperature at the BSR. The temperature required for gas hydrate to be stable at the depth of the BSR is determined using the Canning Seafloor Mound Gen program, which accounts for salinity, gas composition, and pressure effects [*Sloan and Koh*, 2008]. Based on the CTD database, salinity in the Beaufort Sea averages approximately 34.85‰ and varies by no more than 2–3% across the region for water depths where BSRs exist, consistent with observed salinities in the CTD casts and with previously published values [e.g., *Melling*, 1998]. We therefore use seawater salinities in this analysis. We assume a hydrostatic pressure regime and pure methane as the hydrate former, consistent with regional inferences [*Hart et al*., 2011]. We calculate sediment thermal gradients for all the observed BSRs located beneath the seafloor at depths greater than 1000 mbsl and average the thermal gradients for each seismic line every 100 shots (~5 km).

To convert thermal gradient to heat flow, we use regionally measured thermal conductivity values and weighted average values. The thermal conductivities of marine sediments typically vary between 0.8 and 1.6 W/m K [e.g., *Ratcliffe*, 1960] and are controlled by lithology, porosity, pressure, temperature, and the effective thermal properties of the pore-filling fluid (e.g., seawater, gas, or hydrate). Little is known about the sediments on the upper continental slope on the Beaufort margin, although coring programs encountered indurated strata close to the seafloor [*Barnes et al*., 1982]. Assuming porosity values of 35–60% for the upper few hundred meters of ice-free, hemipelagic sediments, combined with direct observations of deepwater conductivities [*Lachenbruch and Marshall*, 1966], we adopted a constant thermal conductivity of 1.1 ± 0.3 W/m K both in the determination of heat flow and in the application of the numerical model. On average, this thermal conductivity value is slightly higher than typical shallow marine sediments (~1 W/m K), but this may be justified because sediments on Arctic Ocean margins are often overconsolidated [e.g., *Hamilton*, 1976; *Reimnitz et al*., 1980; *Reimnitz et al*., 1988].

3.2.3. U.S. Beaufort Sea Heat Flow Map

Interpolating land and sea heat flow results, we produce an initial heat flow map across the U.S. Beaufort Sea (Figure 5). The map shows evidence of moderate heat flow (~40 ± 11 mW m^{-2}) relative to the

surroundings near 146°W, 71°N (approximate shelf break north of Flaxman Island), bordered to the east and west by heat flow values that are nearly 50% higher. The analysis therefore suggests a spatially variable shallow heat flow regime across the Beaufort margin. Currently, we are unable to constrain the cause of this spatially variable heat flow. Deep fluid advection (causing increased heat flow), shallow fluid advection (causing reduced heat flow), and/or variations in sediment thickness and composition, basement morphology, and the degree of attenuation of continental crust may contribute to the inferred pattern of heat flow variability.

3.3. Three-Dimensional Conductive Heat Flow Model

To model steady state methane hydrate stability in the Beaufort Sea at depths shallower than 1000 mbsl, we use a 3-D finite difference scheme that incorporates variable seafloor temperature and accounts for thermal refraction (i.e., lateral variations in the thermal regime caused by variations in bathymetry and boundary conditions across the study area) effects. The approach is identical to previously published 2-D/3-D steady state hydrate stability models [e.g., *Hornbach et al*., 2012; *Phrampus and Hornbach*, 2012]. The 3-D heat flow model has open side boundary conditions, with temperature initially increasing linearly with depth, constant BWT at the top boundary, and a Neumann basal boundary condition defined by the heat flow map (Figure 5). Model resolution, scale, and dimensions as constrained by the legacy USGS seismic lines and by regional multibeam seafloor data [e.g., *Grantz et al*., 1982; *Andreassen et al*., 1995; *Ryan et al*., 2009; *Haxby et al*., 2010] are 20 m in the vertical and 50 m in both horizontal directions.

Ocean water temperature with depth is constrained using 1977 CTD data described in section 3.1. Sediment thermal gradients for each seismic line are imported point by point from the heat flow map (Figure 5). Based on the CTD database, salinity in the Beaufort Sea averages approximately 34.85‰; nonetheless, we account for possible freshwater discharge on the slope or rise [*Dugan and Flemings*, 2000; *Pohlman et al*., 2011] by varying salinity between freshwater (0‰) and the maximum salinity (34.85‰) as part of end-member uncertainty calculations. We then estimate BGHS depth using standard gas hydrate phase boundary methods, assuming pure Structure I methane hydrate [*Sloan and Koh*, 2008].

To extract steady state BGHS depths from the model, we use end-member values that incorporate uncertainties in pore water salinity, pore pressure, heat flow, and velocity-depth uncertainties. Unlike uncertainties in salinity, pressure, and velocity, uncertainties in heat flow vary spatially in the model. All spatial uncertainties are incorporated directly into the BGHS depth estimation to 1 sigma in the model results (Figure 6).

4. BGHS Modeling Results

To compare results for the model-predicted steady state GHSZ with direct observations of BSRs (i.e., the assumed BGHS), we used three seismic profiles: Line 767 in the western U.S. Beaufort Sea and Lines 730 and 718 in the eastern U.S. Beaufort, all of which show clearly observable BSRs (Figures 1 and 6). As expected, a comparison between the predicted steady state BGHS depths and the observed BSRs reveals that the BSRs lie within the predicted BSR zone (calculated assuming uncertainties on input parameters) at water depths greater than the midslope (>1000 mbsl). These are the water depths at which we used a subset of BSR depths to constrain the heat flow map, and as expected, the BSRs are in near steady state conditions in this area. On the upper slope (300–600 mbsl), clear discrepancies exist between predicted and observed BSR depths. In particular, at water depths shallower than ~600 mbsl, observed BSRs are systematically deeper than steady state model predictions (Figure 6). Model results for Lines 718 and 730 (Figures 6a and 6b), which are located within the CMDM (Figure 1), generally match observed BSRs for seafloor depths greater than 1000 mbsl. At shallower depths, predicted steady state BGHS depths and observed BSR depths diverge as the water depth decreases, with the predicted depths systematically shallower than the observed BSRs. Line 767 (Figure 6c), located the farthest west, displays this anomaly as well, but the disparity between observed and predicted BSRs is most pronounced in Lines 718 and 730.

5. Discussion

Multiple phenomena could explain the anomalously deep BSRs observed in seismic data on the upper slope of the U.S. Beaufort Sea margin. Many of the factors that affect the depth of the GHSZ (e.g., variations in pore

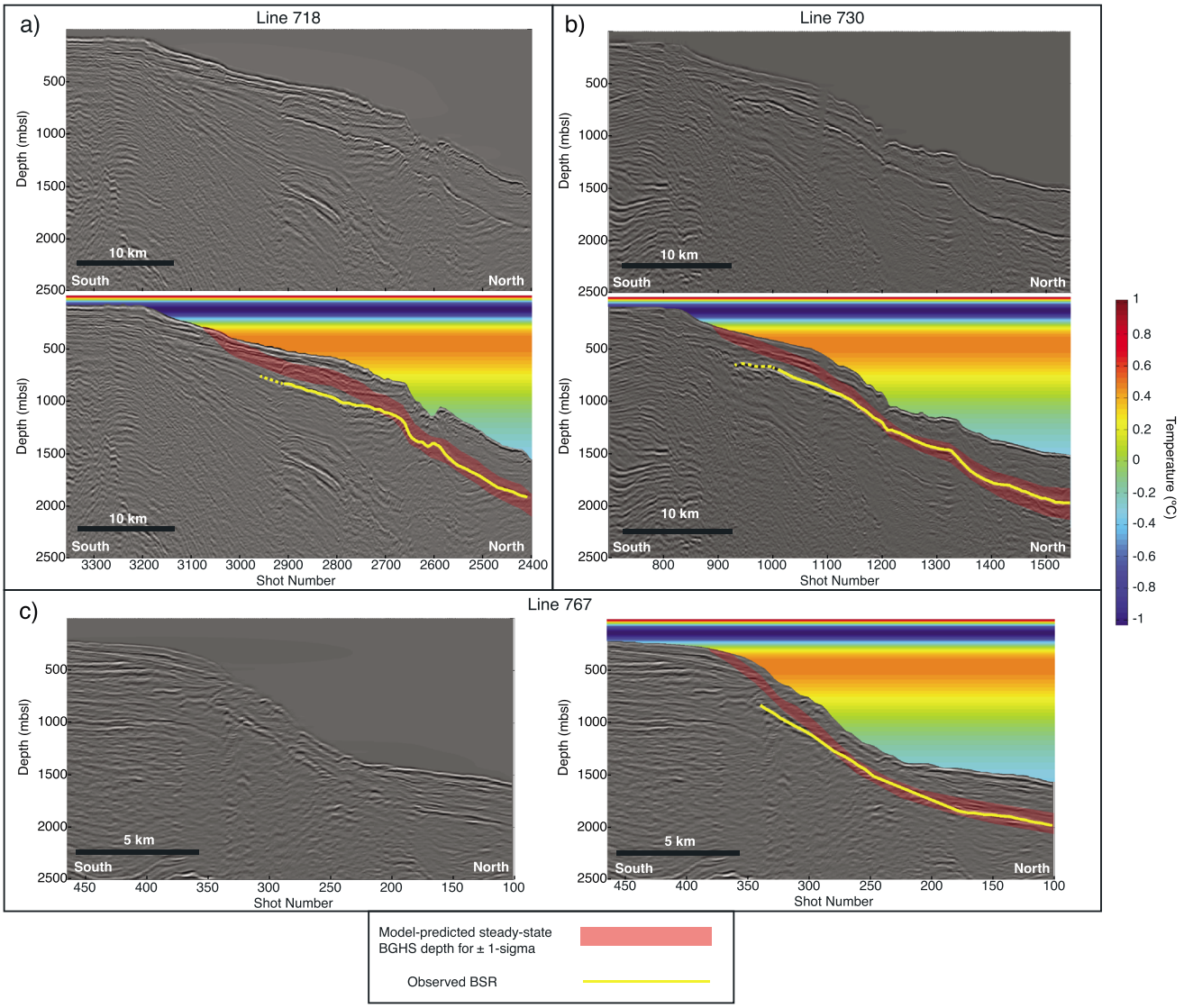

Figure 6. Depth converted seismic lines (a) 718, (b) 730, and (c) 767. For each line, we determine the depth to the BGHS to ±1 sigma (red region), with the observed BSRs marked (yellow). The 1977 Beaufort Sea ocean temperatures are shown for each seismic line. Model-predicted results show that the GHSZ pinches out at 300–350 mbsl. There is a distinct discrepancy between observed and predicted BSRs corresponding to seafloor depths of 300–550 mbsl. Lines (a) 718 and (b) 730 demonstrate this anomaly the best, with line (c) 767 providing a subtler example.

water salinity, velocity-depth uncertainties, and heat flow uncertainty) are already accounted for in the modeling though. We estimate that uncertainties in regional heat flow could be as large as ~35%. Anomalously deep BSRs on the upper continental slope require heat flow to be as much as ~27 mW/m^2 less than the regional estimates (42–56 mW/ m^2), which is significantly larger than our 1 sigma uncertainty of ~15 mW/m^2 (Figure 5). Below, we explore other processes that could explain why observed BSR depths are generally deeper than modeled BGHS depths at seafloor depths of 300–600 m along the upper continental slope on this margin.

5.1. Gas Composition

The guest molecules that are incorporated into gas hydrate strongly affect stability conditions [*Kvenvolden*, 1998; *Sloan and Koh*, 2008] and thus the thickness of the GHSZ. For example, the inclusion of higher-order thermogenic gases (e.g., ethane) in the gas hydrate lattice would cause the BGHS to occur at greater depths than predicted by the model, which assumes Structure I gas hydrate hosting 100% methane. If gases other

than methane were the cause of anomalously deep observed BSRs on the upper continental slope, our analysis implies increasing amounts of higher-order thermogenic gas in the shallow sediments moving up the slope from ~1000 mbsl to ~300 mbsl across the entire U.S. Beaufort Sea margin. We calculate that a mixture of ~15% ethane and ~85% methane by volume would be required to produce observed BSR depths in Lines 718 and 730. A mixture of ~12% ethane and ~88% methane by volume would explain the anomaly observed on Line 767.

Due to the presence of the Barrow Arch, there are clear differences between the maturation of petroleum systems onshore (Alaskan North Slope) and offshore (Beaufort Sea), meaning that it cannot be assumed that world-class deposits like those near Prudhoe Bay extend offshore uninterrupted [*Houseknecht et al*., 2012]. *Houseknecht and Bird* [2011] predict 23 trillion cubic feet (TCF) of gas associated with crude oil and 19 TCF of nonassociated gas under the continental slope. As yet there are no samples confirming these reservoirs nor evidence that these thermogenic gases reach near-seafloor sediments. The only gas hydrate sample recovered from beyond the shelf break on this margin was retrieved not on the upper slope but at ~2500 m water depth above the Canning Seafloor Mound diapiric structure [*Hart et al*., 2011]. Postcruise analysis of residual gas in the core liner revealed >95% methane and less than 1% of strictly thermogenic higher-order hydrocarbons. These results, coupled with carbon isotopic analyses, led *Hart et al*. [2011] to conclude that the gas was either a mixed thermogenic source with some secondary microbial methane or primary microbial methane that had oxidized in the core liner during storage.

5.2. Erosion/Sedimentation Effects

Recent, rapid sedimentation can lead to BSRs that are located at greater depths than steady state models predict [*Ruppel*, 2003; *Martin et al*., 2004; *Hornbach et al*., 2008]. Such BSRs eventually migrate to shallower depths as the sediments undergo thermal reequilibration at a rate controlled by their thermal diffusivity. Currently, the sedimentation rate on the upper continental slope on the U.S. Beaufort margin is poorly constrained. *Reimnitz et al*. [1977] obtained an average sedimentation rate of 0.06 cm yr^{-1} on the U.S. Beaufort shelf, which is far closer to sediment sources than the upper slope, by dividing the observed average thickness of recent (Holocene) sediments (3 m) by the 5 kyr period that their study area had been water covered. *Lewis* [1977] and *Macdonald et al*. [1998] obtained higher rates (0.05 to 0.2 cm yr^{-1} and ~0.8 cm yr^{-1}, respectively) for study areas in Canada near the Mackenzie Delta, which is the only major river on the Beaufort margin. All of these estimates are probably too high to be applied to the entire U.S. Beaufort Sea continental slope and rise, which is currently relatively sediment starved. Nonetheless, we calculate that sedimentation rates of 0.06–0.08 cm/yr will yield heat flow reduction of up to ~2% (~1 mW/m^2) over the course of ~10 kyr, consistent with results in other sedimentary environments [e.g., *Hutchison*, 1985; *Manga et al*., 2012]. This heat flow effect is much too small to explain the disparity between the observed and predicted BSRs.

Rapid or even catastrophic (submarine slides) erosion or sedimentation could strand BSRs at shallower or greater depths, respectively, than would be consistent with contemporary equilibrium conditions. Based on the 1977 USGS seismic data, *Kayen and Lee* [1991] described widespread slope failures on the U.S. Beaufort margin, particularly within the CMDM. To explain the difference in observed and model-predicted BSRs, it requires several hundreds of meters of sediment to have been added recently (during the late Holocene) on the upper slope, but submarine slope failures would have removed, not added, sediment along the upper edge of the margin [e.g., *Kayen and Lee*, 1991]. Thus, slide deposits are an improbable explanation for the anomalously deep BGHS along the upper slope. Additionally, glacial scouring, which affects part of the upper slope in this area [e.g., *Engels et al*., 2008], removes material overlying the BSR. This should lead to anomalously shallow BSRs (not BSRs that are too deep) as the BSRs begin to reequilibrate after the removal of near-seafloor sediments.

5.3. Uplift

Certain patterns of uplift could produce an observed BGHS that is out of equilibrium with present-day ocean temperature structure. As noted in section 2, the U.S. Beaufort Sea margin did not experience continental glaciation during late Pleistocene cold periods [*Dyke et al*., 2002]. Nonetheless, the U.S. Beaufort margin has likely been affected by isostatic rebound in response to the removal of the Laurentide ice sheet (located southeast of the study area) between 10,000 and 14,000 years ago [*Dyke and Prest*, 1987]. Offshore the

Mackenzie River, the uplift associated with rebound reached tens of meters during the late Pleistocene. An additional, although slower, component of uplift to the west within the CMDM is related to the continued northern movement of the Brooks Range [*Mazzotti et al*., 2008; *Houseknecht and Bird*, 2011]. Notably, Lines 718 and 730 through the CMDM display the greatest discrepancy between predicted and observed BSR.

Uplift processes that affect the upper continental slope could change the GHSZ if they resulted in (a) reduced water coverage and thus reduced hydrostatic pressure in the sediments and (b) movement of the seafloor to a shallower, warmer part of the ocean thermocline. In either case, a BSR originally at greater depths within the sediments would readjust to shallower depths to be in equilibrium with present-day conditions. In Lines 718 and 730, the BSR is too deep by a maximum of ~100 and ~250 m, respectively. Constraining the details of the equilibration history of the gas hydrate stability zone following uplift requires better constraints not only on the timing and amount of uplift but also on gas hydrate concentrations and distributions at these sites. Because gas hydrate dissociation is an endothermic process, larger amounts of gas hydrate lead to greater retardation of the dissociation process.

5.4. Offshore Groundwater Discharge

Offshore groundwater discharge from the North Slope of Alaska could potentially enhance hydrate formation on the upper continental slope and potentially explain the observed discrepancy between observed and predicted BSRs. Our model already takes into account the formation of gas hydrate in the presence of fresh pore water as one end-member, and fresh pore water cannot explain the anomalous observed BSRs. In theory, if submarine groundwater discharge from permafrost is cold enough and moves fast enough to transfer fluids from the shelf to the upper slope, this discharge could cool the sediments of the upper slope and deepen the location of the GHSZ. *Deming et al*. [1992] suggested a flow on the order of 0.1 m/yr from the North Slope toward the shelf and slope. We developed a 2-D advection-diffusion model for groundwater discharge perpendicular to the coast (supporting information). Our results show that a flow of ~0.2 m/yr from the shelf to the upper slope could in theory explain the anomalously deep BGHS we observe on the upper slope; however, this explanation requires a physically unreasonable 1600 m thick cold water (~0°C) plume to migrate laterally toward the upper slope (Figure S1 in the supporting information). Such a plume would substantially reduce observed terrestrial heat flow values [e.g., *Deming et al*., 1992]. Alternatively, we can model a thinner groundwater plume that explains anomalously deep BSRs along the U.S. Beaufort Sea upper slope, but doing so requires flow rates a factor of 5 or more larger than previous models suggest [*Deming et al*., 1992].

5.5. Intermediate Ocean Temperature Changes

A plausible explanation for the discrepancy between observed and predicted BSR depths on parts of the Beaufort upper continental slope shallower than 1000 mbsl is that BWT has not been constant [e.g., *Melling*, 1998; *Dmitrenko et al*., 2009]. Our analysis of ocean temperature change results shows evidence for multidecadal ocean warming (up to 39 years) of ~0.5°C in the Beaufort Sea at water depths of 300–550 mbsl (Figure 4). Uncertainties in mean annual ocean temperature and mean annual change in ocean temperature are high in waters shallower than ~300 mbsl, which is updip of the current depth at which methane hydrate could be stable. These uncertainties are attributed to large, high-frequency, intraannual ocean temperature variations that result in large uncertainty in the multidecadal temperature variation analysis [e.g., *Pickart*, 2004]. At depths greater than ~300 mbsl, however, we observe less uncertainty in average intraannual temperatures (Figure 4). Lower uncertainty combined with significant changes in average annual temperature provide statistically significant evidence (greater than 2 sigma) for annual ocean temperature warming at depths between 300 and 550 mbsl in the U.S. Beaufort Sea, directly coincident with anomalous BSR depths on the upper slope (Figures 4 and 6). Additionally, between 300 and 600 mbsl, the Monte Carlo analysis indicates a positive slope of more than 75% of the realizations for both winter-spring and summer-fall data sets (Figure 3), implying clear and statistically significant mean ocean temperature warming at these depths during this time period (Figure 4).

These results are consistent with previous studies indicating intermediate water depth warming in other parts of the Arctic over shorter time scales (300–500 mbsl) [e.g., *Melling*, 1998; *Shimada et al*., 2004; *Dmitrenko et al*., 2009; *McLaughlin et al*., 2009; *Westbrook et al*., 2009]. Such warming has been traced to warming of

Atlantic waters, which travel counterclockwise around the edges of the Arctic Ocean basin before reaching the Beaufort Sea, where there underlie Pacific waters [e.g., *Melling*, 1998; *Pickart*, 2004; *Dmitrenko et al*., 2009].

We suggest that multidecadal ocean temperature warming of at least 1°C is the primary reason we observe a discrepancy between observed and predicted BSRs in the Beaufort Sea. Anomalously deep BSRs observed on the upper continental slope may still be adjusting to intermediate ocean temperature warming at multidecadal scales. Therefore, the anomalously deep BSRs observed on the upper slope likely represent paleo-BSRs that have yet to equilibrate to the warming BWT. Ocean temperature warming alone is not enough to explain all discrepancies between observed and predicted BSRs. For observed BSRs to be in steady state equilibrium requires BWT as cold as −2.3°C on the upper continental slope (300 to 550 mbsl), a temperature that is lower than the freezing point of seawater (−2°C) and colder than the lowest inferred benthic temperatures for the late Quaternary based on the analyses of benthic foraminifera [e.g., *Waelbroeck et al*., 2002]. Therefore, although multidecadal ocean temperature warming plays an important role in ongoing destabilization of methane hydrate on the upper slope on the U.S. Beaufort Sea margin, other factors (e.g., groundwater discharge and/or uplift) could contribute to gas hydrate dynamics across this region.

5.6. Implications

Regardless of the exact cause of the disparity between the predicted and observed BSR depths on the Beaufort slope, the necessary reequilibration of the BGHS with time due to multidecadal, intermediate ocean temperature warming requires ongoing and future hydrate dissociation along a potentially significant portion of the continental margin. Based on our preliminary analysis of the location of anomalous BSRs, we suggest that the zone of hydrate instability is 10 to 15 km wide in the along-slope direction on the upper continental slope along much of the U.S. Beaufort margin. Using these bounds, we estimate that ~5–7.5 × 10^3 km^2 could contain gas hydrates that are currently subject to dissociation on the upper slope. Over a 10 km wide swath of the upper slope, the seafloor deepens from 325 m to more than 575 m, while the theoretical GHSZ thickens from ~0 m to more than 200 m. If the thickness of sediments containing gas hydrate on the upper slope is taken as an average of 100 m, then the total sediment volume hosting potentially dissociating gas hydrates is in the range of ~5 to 7.5 × 10^{11} m^3. Assuming an average porosity of 30–50% and hydrate filling 2.5–5% of the available pore space (similar to Blake Ridge [*Holbrook et al*., 1996]), and methane accounting for 12.9% by weight in Structure I gas hydrate, we estimate that ~0.44 to 2.2 Gt of methane, containing 0.33 to 1.65 Gt carbon, is currently destabilizing on the U.S. Beaufort Sea upper slope. The estimate scales linearly with changes in porosity, gas hydrate saturation in pore space, and the thickness of the hydrate-bearing zone. For example, for 50% porosity and 5% hydrate saturation in pore space and with an average stability zone thickness of 150 m over a 15 km wide swath of the upper slope, the upper bound estimate would increase by 1.5 times to ~2.48 Gt C in currently dissociating deposits. Further analysis and particularly in situ sampling (e.g., ocean drilling) are necessary to validate these estimates and the field parameters that are involved in the calculations.

The rate of dissociation of upper slope gas hydrates is unknown but has implications for the time scale at which these susceptible deposits respond to climate warming. On the U.S. Atlantic margin, an analysis of bubble sizes and emission rates observed at a handful of seeps was scaled up to yield an estimate of 15–90 Mg yr^{-1} CH_4 released at the seafloor [*Skarke et al*., 2014]. Applying the upper bound emission rate to the U.S. Beaufort margin and assuming that the seafloor emission represents 10% of the gas released from dissociating methane hydrates (i.e., 80% consumed by oxidation in the sediments and another 10% retained in pore space), nearly 10^6 year would be required for complete breakdown of the lower bound estimate for upper slope gas hydrate on the U.S. Beaufort margin. This is unreasonably long given the dramatic climate change events that occur over time scales as short as 2 × 10^4 years. Another way to assess dissociation rates is to determine how much methane would be released at the seafloor if all of the upper slope gas hydrates in a 10 km swath on the U.S. Beaufort Sea margin were to dissociate over 100 or 500 year. Again assuming that only 10% of the released methane reaches the seafloor, the emission rates would be ~440 Gg yr^{-1} and 88 Gg yr^{-1} for 100 and 500 year dissociation episodes, respectively, for the case of 30% formation porosity and 2.5% hydrate saturation in pore space. These values are orders of magnitude higher than the emission rates estimated based on northern U.S. Atlantic margin seepage studies [*Skarke et al*., 2014]. Future studies should focus on

gathering direct evidence for upper slope gas hydrate dissociation and seepage to provide constraints on the location and rates of these processes.

The sediment thickness above the BSRs along the upper slope on the U.S. Beaufort margin is generally less than 250 m at most locations. The corresponding height of the gas column necessary to trigger fault reactivation, gas migration, and possible slope failure [*Kayen and Lee*, 1991; *Hornbach et al*., 2004] is therefore only a few tens of meters, assuming that the gas in the pores is interconnected. Our analysis therefore suggests an increased likelihood of slope failure along the upper slope in the coming century as gas hydrates continue to warm and dissociate across this region due to ocean temperature warming.

6. Conclusions

BSRs located beneath the U.S. Beaufort Sea continental slope appear too deep to coincide with a BGHS in steady state equilibrium. The cause of anomalously deep BSRs on the upper slope of the U.S. Beaufort Sea margin is uncertain and could reflect a combination of processes. Nonetheless, the observation of multidecadal ocean temperature warming at intermediate water depths provides at least a partial explanation for anomalously deep BSRs on the upper slope in this area. Our analysis of multidecadal variations in ocean temperatures reveals clear warming at intermediate depths (~300–550 mbsl). This warming requires some methane hydrates on the U.S. Beaufort Sea upper slope to destabilize and the BGHS to migrate to shallower depths to reach equilibrium in the future. The zone in which the BGHS is actively reequilibrating may cover an area of at least 5000 km^2. Even in the absence of continued future ocean warming, we conservatively estimate that ~0.44 to 2.2 Gt CH_4 will be released from gas hydrate into the sediments in the coming decades to centuries due to intermediate ocean temperature warming that has already occurred over the last ~39 years. This dissociation could promote slope failure by reducing sediment strength. If the gas were eventually released from the sediments at the seafloor above the dissociating gas hydrates, it would not be expected to reach the sea surface, instead dissolving in ocean waters [*McGinnis et al*., 2006] and oxidizing to CO_2 [*Mau et al*., 2007]. If some of the gas migrates updip and is emitted at the shelf break (~100 m), a fraction could reach the atmosphere directly [*McGinnis et al*., 2006].

The approach outlined here has applicability beyond the U.S. Beaufort Sea margin. Globally, the most climate-sensitive part of the deepwater gas hydrate system lies within the sediments of the upper continental slopes [*Kvenvolden*, 1993; *Ruppel*, 2011], where the GHSZ thins to nearly zero thickness and where intermediate ocean waters impinge. Other studies indicate that upper continental slope gas hydrate degradation may be relatively widespread on passive margins (e.g., Svalbard margin [*Westbrook et al*., 2009] and the U.S. Atlantic margin [*Phrampus and Hornbach*, 2012; *Brothers et al*., 2014; *Skarke et al*., 2014]). The application of the steady state 3-D thermal model in both high and middle-to-low-latitude areas will contribute to an understanding of the global distribution of gas hydrates that are out of equilibrium with present-day ocean temperature conditions.

Acknowledgments

This work was supported by the U.S. Department of Energy (DOE), grant DE-FE0010180 to SMU and a USGS-DOE interagency agreement DE-FE0005806. Any use of trade, firm, or product names is for descriptive purposes only and does not imply endorsement by the U.S. Government. All data used in this analysis are publically available. The 1977 MCS data were obtained from the USGS, heat flow data from previously published works, and CTD data from the World Ocean Database.

References

Allen, D. M., F. A. Michel, and A. S. Judge (1988), The permafrost regime in the Mackenzie Delta, Beaufort Sea region, N.W.T. and its significance to the reconstruction of the palaeoclimatic history, *J. Quat. Sci.*, *3*(1), 3–13.

Andreassen, K., P. E. Hart, and A. Grantz (1995), Seismic studies of a bottom simulating reflection related to gas hydrate beneath the continental margin of the Beaufort Sea, *J. Geophys. Res.*, *100*(B7), 12,659–12,673, doi:10.1029/95JB00961.

Andreassen, K., P. E. Hart, and M. MacKay (1997), Amplitude versus offset modeling of the bottom simulating reflection associated with submarine gas hydrates, *Mar. Geol.*, *137*, 25–40.

Archer, D. (2007), Methane hydrate stability and anthropogenic climate change, *Biogeosci. Discuss.*, *4*(2), 993–1057.

Barnes, P. W., E. Reimnitz, and D. Fox (1982), Ice rafting of fine-grained sediment, a sorting and transport mechanism, Beaufort Sea, Alaska, *J. Sediment. Res.*, *52*(2), 493–502.

Biastoch, A., et al. (2011), Rising Arctic Ocean temperatures cause gas hydrate destabilization and ocean acidification, *Geophys. Res. Lett.*, *38*, L08602, doi:10.1029/2011GL047222.

Blasco, S., et al. (2011), 2010 State of Knowledge: Beaufort sea seabed geohazards associated with offshore hydrocarbon development, *Geol. Surv. of Can. Open File 6989*, 335, doi:10.4095/292616.

Brigham, J. K., and G. H. Miller (1983), Paleotemperature estimates of the Alaskan Arctic Coastal Plain during the last 125,000 years, in *Proceedings of the 4th International Conference on Permafrost*, pp. 80–85, Natl. Acad. Press, Washington, D. C.

Brothers, D., C. Ruppel, J. Kluesner, U. Brink, J. Chaytor, J. Hill, B. Andrews, and C. Flores (2014), Seabed fluid expulsion along the upper slope and outer shelf of the US Atlantic continental margin, *Geophys. Res. Lett.*, *41*, 96–101, doi:10.1002/2013GL058048.

Brothers, L. L., P. E. Hart, and C. D. Ruppel (2012), Minimum distribution of subsea ice-bearing permafrost on the US Beaufort Sea continental shelf, *Geophys. Res. Lett.*, *39*, L15501, doi:10.1029/2012GL052222.

Camilli, R., C. M. Reddy, D. R. Yoerger, B. A. Van Mooy, M. V. Jakuba, J. C. Kinsey, C. P. McIntyre, S. P. Sylva, and J. V. Maloney (2010), Tracking hydrocarbon plume transport and biodegradation at Deepwater Horizon, *Science*, *330*(6001), 201–204.
Carmack, E., R. Macdonald, and J. Papadakis (1989), Water mass structure and boundaries in the Mackenzie shelf estuary, *J. Geophys. Res.*, *94*(C12), 18,043–18,055, doi:10.1029/JC094iC12p18043.
Collett, T., Geological Survey (U.S.), Morgantown Energy Research Center, and United States Department of Energy (1988), Geologic interrelations relative to gas hydrates within the North Slope of Alaska, U.S. Department of the Interior, Geological Survey.
Deming, D., J. H. Sass, A. H. Lachenbruch, and R. F. De Rito (1992), Heat flow and subsurface temperature as evidence for basin-scale groundwater flow, North Slope of Alaska, *Geol. Soc. Am. Bull.*, *104*, 528–542.
Dickens, G. R., J. R. O'Neil, D. K. Rea, and R. M. Owen (1995), Dissociation of oceanic methane hydrate as a cause of the carbon isotope excursion at the end of the Paleocene, *Paleooceanography*, *10*(6), 965–971.
Dix, C. H. (1955), Seismic velocities from surface measurements, *Geophysics*, *20*(1), 68–86.
Dmitrenko, I. A., et al. (2009), Seasonal modification of the Arctic Ocean intermediate water layer off the eastern Laptev Sea continental shelf break, *J. Geophys. Res.*, *114*, C06010, doi:10.1029/2008JC005229.
Dugan, B., and P. B. Flemings (2000), Overpressure and fluid flow in the New Jersey continental slope: Implications for slope failure and cold seeps, *Science*, *289*(5477), 288–291.
Dyke, A. S., and V. K. Prest (1987), Late Wisconsinan and Holocene history of the Laurentide ice sheet, *Géogr. Phys. et Quat.*, *41*(2), 237–263.
Dyke, A. S., J. T. Andrews, P. U. Clark, J. H. England, G. H. Miller, J. Shaw, and J. J. Veillette (2002), The Laurentide and Innuitian ice sheets during the last glacial maximum, *Quat. Sci. Rev.*, *21*(1), 9–31.
Engels, J. L., M. H. Edwards, L. Polyak, and P. D. Johnson (2008), Seafloor evidence for ice shelf flow across the Alaska–Beaufort margin of the Arctic Ocean, *Earth Surf. Processes Landforms*, *33*(7), 1047–1063.
Flemings, P. B., X. Liu, and W. J. Winters (2003), Critical pressure and multiphase flow in Blake Ridge gas hydrates, *Geology*, *31*, 1057–1060.
Grantz, A., G. Boucher, and O. T. Whitney (1976), Possible solid gas hydrate and natural gas deposits beneath the continental slope of the Beaufort Sea, *U.S. Geol. Surv. Circular, 733*, 17.
Grantz, A., D. M. Mann, and S. D. May (1982), Tracklines of multichannel seismic-reflection data collected by the US Geological Survey in the Beaufort and Chukchi Seas in 1977 for which profiles and stack tapes are available, *U.S. Geol. Surv. Open File Rep.*, 82–0735.
Grantz, A., S. May, and P. Hart (1990), Geology of the Arctic continental margin of Alaska, *Geol. North Am.*, *50*, 257–288.
Hamilton, E. L. (1976), Variations of density and porosity with depth in deep-sea sediments, *J. Sediment. Res.*, *46*(2), 280–300.
Hart, P. E., J. W. Pohlman, T. D. Lorenson, and B. D. Edwards (2011), Beaufort Sea Deep-water gas hydrate recovery from a seafloor mound in a region of widespread BSR occurence, in *Proceedings of the 7th International Conference on Gas Hydrates (ICGH 2011)*, Edinburgh, Scotland.
Haxby, W., A. Melkonian, J. Coplan, S. Chan, and W. Ryan (2010), GeoMapApp freeware software, v. 2.3, Lamont-Doherty Earth Observatory, Palisades. [Available at http://jgs.geoscienceworld.org/cgi/content/full/168/2/333].
Holbrook, W. S., H. Hoskins, W. T. Wood, R. A. Stephen, and D. Lizarralde (1996), Methane hydrate and free gas on the blake ridge from vertical seismic profiling, *Science*, *273*(5283), 1840–1843.
Hornbach, M. J., D. M. Saffer, and W. S. Holbrook (2004), Critically pressured free-gas reservoirs below gas-hydrate provinces, *Nature*, *427*, 142–144.
Hornbach, M. J., D. M. Saffer, W. S. Holbrook, H. J. Van Avendonk, and A. R. Gorman (2008), Three-dimensional seismic imaging of the Blake Ridge methane hydrate province: Evidence for large, concentrated zones of gas hydrate and morphologically driven advection, *J. Geophys. Res.*, *113*, B07101, doi:10.1029/2007JB005392.
Hornbach, M. J., N. L. Bangs, and C. Berndt (2012), Detecting hydrate and fluid flow from bottom simulating reflector depth anomalies, *Geology*, *40*(3), 227–230.
Houseknecht, D. W., and K. J. Bird (2006), Oil and gas resources of the Arctic Alaska petroleum province, *U.S. Geol. Surv. Prof. Pap.*, 1732–A.
Houseknecht, D. W., and K. J. Bird (2011), Geology and petroleum potential of the rifted margins of the Canada Basin, *Geol. Soc. London Mem.*, *35*(1), 509–526.
Houseknecht, D., W. Burns, and K. Bird (2012), Thermal maturation history of Arctic Alaska and the southern Canada basin, Analyzing the Thermal History of Sedimentary Basins.
Hutchison, I. (1985), The effects of sedimentation and compaction on oceanic heat flow, *Geophys. J. R. Astron. Soc.*, *82*, 439–459.
Johannessen, O. M., et al. (2004), Arctic climate change: Observed and modelled temperature and sea-ice variability, *Tellus*, *56A*, 328–341.
Kayen, R. E., and H. J. Lee (1991), Pleistocene slope instability of gas hydrate laden sediment on the Beaufort sea margin, *Mar. Geotechnol.*, *10*(1–2), 125–141.
Kvenvolden, K. A. (1988), Methane hydrate-a major reservoir of carbon in the shallow geosphere?, *Chem. Geol.*, *71*(1), 41–51.
Kvenvolden, K. A. (1993), Gas hydrates—geological perspective and global change, *Rev. Geophys.*, *31*(2), 173–187, doi:10.1029/93RG00268.
Kvenvolden, K. A. (1998), A primer on the geological occurrence of gas hydrate, *Geol. Soc. London Spec. Publ.*, *137*(1), 9–30.
Kvenvolden, K. A., and A. Grantz (1990), Gas hydrates of the Arctic Ocean region, in *The Arctic Ocean Region, Geology of North America*, pp. 539–549, Geol. Soc. Am., Boulder, Colo.
Lachenbruch, A., and B. V. Marshall (1966), Heat flow through the Arctic Ocean floor: The Canada Basin-Alpha Rise Boundary, *J. Geophys. Res.*, *71*(4), 1223–1248, doi:10.1029/JZ071i004p01223.
Lachenbruch, A., and B. V. Marshall (1969), Heat flow in the Arctic, *Arctic*, *22*(3), 300–311.
Lachenbruch, A., J. H. Sass, B. V. Marshall, and T. H. Moses Jr. (1982), Permafrost, heat flow, and the Geothermal Regime at Prudhoe Bay, Alaska, *J. Geophys. Res.*, *87*(B11), 9301–9316, doi:10.1029/JB087iB11p09301.
Levitus, S., T. P. Boyer, M. E. Conkright, T. O'Brien, J. Antonov, C. Stephens, L. Stathoplos, D. Johnson, and R. Gelfeld (1998), NOAA Atlas NESDIS 18, World Ocean Database 1998: vol. 1: Introduction, 346 pp., Natl. Oceanic and Atmos. Admin., Silver Spring, Md.
Lewis, C. F. M. (1977), Bottom scour by sea ice in the southern Beaufort Sea. Dept. of Fisheries and the Environment, Beaufort Sea Tech. Rep. 23 (draft), Beaufort Sea Project, Victoria, British Columbia, 88.
Macdonald, R., S. Solomon, R. Cranston, H. Welch, M. Yunker, and C. Gobeil (1998), A sediment and organic carbon budget for the Canadian Beaufort Shelf, *Mar. Geol.*, *144*(4), 255–273.
Manga, M., et al. (2012), Heat flow in the Lesser Antilles island arc and adjacent back arc Grenada basin, *Geochem., Geophys., Geosyst.*, *13*, Q08007, doi:10.1029/2012GC004260.
Marín-Moreno, H., T. A. Minshull, G. K. Westbrook, B. Sinha, and S. Sarkar (2013), The response of methane hydrate beneath the seabed offshore Svalbard to ocean warming during the next three centuries, *Geophys. Res. Lett.*, *40*, 5159–5163, doi:10.1002/grl.50985.
Martin, V., P. Henry, H. Nouze, M. Noble, J. Ashi, and G. Pascal (2004), Erosion and sedimentation as processes controlling the BSR-derived heat flow on the Eastern Nankai margin, *Earth Planet. Sci. Lett.*, *222*(1), 131–144.

Mau, S., D. L. Valentine, J. F. Clark, J. Reed, R. Camilli, and L. Washburn (2007), Dissolved methane distributions and air-sea flux in the plume of a massive seep field, Coal Oil Point, California, *Geophys. Res. Lett.*, *34*, L22603, doi:10.1029/2007GL031344.
Mazzotti, S., L. J. Leonard, R. D. Hyndman, and J. F. Cassidy (2008), Tectonics, dynamics, and seismic hazard in the Canada-Alaska Cordillera, in *Active Tectonics and Seismic Potential of Alaska*, pp. 297–319, AGU, Washington, D. C.
McGinnis, D., J. Greinert, Y. Artemov, S. Beaubien, and A. Wüest (2006), Fate of rising methane bubbles in stratified waters: How much methane reaches the atmosphere?, *J. Geophys. Res.*, *111*, C09007, doi:10.1029/2005JC003183.
McLaughlin, F., E. C. Carmack, W. J. Williams, S. Zimmermann, K. Shimada, and M. Itoh (2009), Joint effects of boundary currents and thermohaline intrusions on the warming of Atlantic water in the Canada Basin, 1993–2007, *J. Geophys. Res.*, *114*, C00A12, doi:10.1029/2008JC005001.
Melling, H. (1998), Hydrographic changes in the Canada Basin of the Arctic Ocean, 1979–1996, *J. Geophys. Res.*, *103*(C4), 7637–7645, doi:10.1029/97JC03723.
Osterkamp, T., and M. Payne (1981), Estimates of permafrost thickness from well logs in northern Alaska, *Cold Reg. Sci. Technol.*, *5*(1), 13–27.
Osterkamp, T., J. Petersen, and T. Collet (1985), Permafrost thicknesses in the Oliktok point, Prudhoe Bay and Mikkelsen Bay areas of Alaska, *Cold Reg. Sci. Technol.*, *11*(2), 99–105.
Paul, L. E. (1994), Geological, Geochemical, and Operational Summary, Aurora Well, OCS Y-0943-1, Beaufort Sea, Alaska, US Department of the Interior, Minerals Management Service, Alaska OCS Region.
Paull, C. K., W. Ussler III, S. R. Dallimore, S. M. Blasco, T. D. Lorenson, H. Melling, B. E. Medioli, F. M. Nixon, and F. A. McLaughlin (2007), Origin of pingo-like features on the Beaufort Sea shelf and their possible relationship to decomposing methane gas hydrates, *Geophys. Res. Lett.*, *34*, L01603, doi:10.1029/2006GL027977.
Phrampus, B. J., and M. J. Hornbach (2012), Recent changes to the Gulf Stream causing widespread gas hydrate destabilization, *Nature*, *490*, 527–530, doi:10.1038/nature11528.
Pickart, R. S. (2004), Shelfbreak circulation in the Alaskan Beaufort Sea: Mean structure and variability, *J. Geophys. Res.*, *109*, C04024, doi:10.1029/2003JC001912.
Pohlman, J., T. Lorenson, P. Hart, C. Ruppel, C. Joseph, M. Torres, and B. Edwards (2011), Evidence for freshwater discharge at a gas hydrate-bearing seafloor mound on the beaufort sea continental slope, paper presented at AGU Fall Meeting, San Francisco, Calif., 5–9 Dec.
Ratcliffe, E. (1960), The thermal conductivities of ocean sediments, *J. Geophys. Res.*, *65*(5), 1535–1541, doi:10.1029/JZ065i005p01535.
Reagan, M. T., G. J. Moridis, S. M. Elliott, and M. Maltrud (2011), Contribution of oceanic gas hydrate dissociation to the formation of Arctic Ocean methane plumes, *J. Geophys. Res.*, *116*, C09014, doi:10.1029/2011JC007189.
Reeburgh, W. S. (2007), Oceanic methane biogeochemistry, *Chem. Rev.*, *107*(2), 486–513.
Reimnitz, E., P. Barnes, L. Toimil, and J. Melchior (1977), Ice gouge recurrence and rates of sediment reworking, Beaufort Sea, Alaska, *Geology*, *5*(7), 405–408.
Reimnitz, E., E. Kempema, R. Ross, and P. Minkler (1980), Overconsolidated surficial deposits on the Beaufort Sea shelf, U.S. Geol. Surv.
Reimnitz, E., S. M. Graves, and P. W. Barnes (1988), Beaufort Sea coastal erosion, sediment flux, shoreline evolution, and the erosional shelf profile, U.S. Geol. Surv.
Ruppel, C. (1997), Anomalously cold temperatures observed at the base of the gas hydrate stability zone on the U.S. Atlantic passive margin, *Geology*, *25*(8), 699–702.
Ruppel, C. (2003), Thermal state of the gas hydrate reservoir, in *Natural Gas Hydrate in Oceanic and Permafrost Environments*, edited by M. D. Max, pp. 29–42, Springer, Dordrecht, Netherlands.
Ruppel, C. (2011), Methane hydrates and contemporary climate change, *Nat. Educ. Knowl.*, *3*(10), 29.
Ruppel, C., and M. Kinoshita (2000), Fluid, methane, and energy flux in an active margin gas hydrate province, offshore Costa Rica, *Earth Planet. Sci. Lett.*, *179*(1), 153–165.
Ruppel, C., R. P. Von Herzen, and A. Bonneville (1995), Heat flux through an old (−175 Ma) passive margin: Offshore southeastern United States, *J. Geophys. Res.*, *100*(B10), 20,037–20,057, doi:10.1029/95JB01860.
Ryan, W. B., S. M. Carbotte, J. O. Coplan, S. O'Hara, A. Melkonian, R. Arko, R. A. Weissel, V. Ferrini, A. Goodwillie, and F. Nitsche (2009), Global Multi-Resolution Topography synthesis, *Geochem. Geophys. Geosyst.*, *10*, Q03014, doi:10.1029/2008GC002332.
Shakhova, N., I. Semiletov, A. Salyuk, V. Yusupov, D. Kosmach, and Ö. Gustafsson (2010), Extensive methane venting to the atmosphere from sediments of the East Siberian Arctic Shelf, *Science*, *327*(5970), 1246–1250.
Shimada, K., F. McLaughlin, E. Carmack, A. Proshutinsky, S. Nishino, and M. Itoh (2004), Penetration of the 1990s warm temperature anomaly of Atlantic Water in the Canada Basin, *Geophys. Res. Lett.*, *31*, L20301, doi:10.1029/2004GL020860.
Shipley, T. H., M. H. Houston, R. T. Buffler, F. J. Shaub, K. J. McMillen, J. W. Ladd, and J. L. Worzel (1979), Seismic evidence for widespread possible gas hydrate horizons on continental slopes and rises, *AAPG Bull.*, *63*(12), 2204–2213.
Skarke, A., C. Ruppel, M. Kodis, D. Brothers, and E. Lobecker (2014), Widespread methane leakage from the sea floor on the northern US Atlantic margin, *Nat. Geosci.*, *7*, 657–661.
Sloan, E. D., and C. A. Koh (2008), *Clathrate Hydrates of Natural Gases*, 3rd ed., CRC Press, Boca Raton, Fla.
Waelbroeck, C., L. Labeyrie, E. Michel, J. C. Duplessy, J. McManus, K. Lambeck, E. Balbon, and M. Labracherie (2002), Sea-level and deep water temperature changes derived from benthic foraminifera isotopic records, *Quat. Sci. Rev.*, *21*(1), 295–305.
Westbrook, G. K., K. E. Thatcher, E. J. Rohling, A. M. Piotrowski, H. Pälike, A. H. Osborne, E. G. Nisbet, T. A. Minshull, M. Lanoisellé, and R. H. James (2009), Escape of methane gas from the seabed along the West Spitsbergen continental margin, *Geophys. Res. Lett.*, *36*, L15608, doi:10.1029/2009GL039191.
Yamano, M., S. Uyeda, Y. Aoki, and T. H. Shipley (1982), Estimates of heat flow derived from gas hydrates, *Geology*, *10*(7), 339–343.